TALENTA Conference Series: Energy and Engineering (EE)

PAPER – OPEN ACCESS

The Use Of Seismic Energy And Damage Index For Assesment Seismic Performance Of Building Under Seismic Excitation

Author : Daniel Rumbi Teruna
DOI : 10.32734/ee.v1i1.125
ISSN : 2654-7031
E-ISSN : 2654-704X

Volume 1 Issue 1 – 2018 TALENTA Conference Series: Energy and Engineering

EE Conference Series 01 (2018), Page 145-153

TALENTA Conference Series

Available online at https://talentaconfseries.usu.ac.id

The Use Of Seismic Energy And Damage Index For Assesment Seismic Performance Of Building Under Seismic Excitation

Daniel Rumbi Teruna [a]*

[a]*Faculty of Engineering, University of Sumatera Utara, 20155, Indonesia*
danielteruna@yahoo.com,danielteruna@usu.ac.id

Abstract

Seismic input energy is transmitted into building consists of the kinetic energy, elastic strain energy, damping energy, and hysteretic energy. The amount of the input energy induced by earthquake transmitted into a building depends on earthquake characteristics and building dynamic properties. In this context, the hysteretic energy directly associated with damage to structural members through a parameter which known as the damage index were introduced. For this purposes, influence of earthquake characteristic on energy spectra for SDOF system were described and presented. In addition, influence of structural dynamic properties are also described and discussed. Next, to assess the damage potential to a building under seismic excitation, four story steel moment resisting frame were investigated under three selected ground motion records matching to the response spectra design the new Indonesian code. Furthermore, nonlinear dynamic time history analysis were performed using ABAQUS to obtain responses parameters in term of base shear, drift, input and hysteretic energy. Finally, the seismic performance of the building based on Park and Ang damage index model is presented and summarized.

Keywords: excitation; energy; nonlinear; responses parameter; performance;

1. Introduction

In the past twenty years, the general philosophy for seismic-resistant design of structures has undergone some changes, since some of the most destructive earthquakes shock all over the world The conventional elastic force-based design methodology based on acceleration spectra is gradually getting replaced by more rational seismic design approaches such as: displacement based design method [3], and energy design concept [4][6]. Seismic response of structures under seismic excitation may be characterized in terms of distribution of seismic input energy transmitted into the structure and its various energy components versus time. The seismic input energy of a system consists of kinetic energy, viscous damping energy, hysteretic energy and elastic strain energy [11][10]. Kinetic energy reflects the work of the inertia fore, while elastic strain energy is stored in the system in the form of elastic strain. Both of these energy occurs in the initial stages of the earthquake and vanish as the structure come to rest. Furthermore, damping energy reflects the work of damping force and hysteretic energy is the portion of the input energy dissipated by hysteretic action. The last two term of these energy have maximum value at the end of the earthquake and these energy are irrecoverable. The input energy account for the earthquake characteristics (frequency content, intensity, and duration of strong motion) and structure characteristics (period, ductility, damping, and hysteretic behavior).

Selection and peer-review under responsibility of Seminar Ilmiah Nasional Dies Natalis USU-64

Therefore, to investigate the damage potential of structure under ground motion excitation, it is necessary to understand the estimation, and correlation seismic input energy to responses quantity of structure.

2. Seismic Energy

2.1. Energy Balance Equation

The differential equation of motion for a nonlinear SDOF system subjected to earthquake ground motion is expressed as [10].

$$m\ddot{u}(t) + c\dot{u}(t) + f_s(u, \dot{u}) = -m\ddot{u}_g(t) \quad (1)$$

where m is mass of the system, c is the damping coefficient, f_s is the restoring force, $\ddot{u}$,$\dot{u}$ and u are acceleration, velocity, and displacement with respect to ground respectively, $\ddot{u}_g$ is ground motion acceleration, and t is time. The energy balance equation is obtained by integrating the each term in Eq.(1) over an increment of global structural displacements (du), the equation lead to:

$$\int m\dot{u}d\dot{u} + \int c\dot{u}du + \int f_s\,du = -\int m\ddot{u}_g\,du \quad (2)$$

Refer to Eq.(6), energy balance equation is can be written in simply form as

$$E_k(t) + E_{vd}(t) + E_a(t) = E_i(t) \quad (3)$$

where $E_k(t)$ denotes the relative kinetic energy, $E_{vd}(t)$ is the energy dissipated by viscous damping, $E_a(t)$ is the absorbed energy, Ed(t) is the energy dissipated by passive damper, $E_i(t)$ and is the relative input energy such that

$$E_k(t) = \int m\dot{u}d\dot{u} = \frac{1}{2}m\dot{u}^2 \quad (4)$$

$$E_{vd}(t) = \int c\dot{u}du \quad (5)$$

$$E_a(t) = \int f_s\,du \quad (6)$$

$$E_i(t) = \int m\ddot{u}_g\,du \quad (7)$$

The absorbed energy $E_a(t)$ is the total amount of energy absorbed by structural component that consist of recoverable absorbed energy through elastic straining and unrecoverable absorbed energy through inelastic deformation its component. Thus,

$$E_a(t) = E_s(t) + E_h(t) \quad (8)$$

where $E_s(t)$ is the recoverable elastic strain energy and $E_h(t)$ is the energy dissipated through hysteretic damping.

2.2. Influence of Ground Motion Characteristic And Structural Properties On Energy Spectra

2.2.1. Influence of peak ground acceleration

Figure 1 presents the input energy spectra of Northridge earthquake of Arleta Nordhoff fire station with PGA = 0.4g, 0.6g, and 0,8g. The figure were constructed for SDOF system with strength ratio $\eta = Q_y/mPGA = 0.2$, and damping ratio $\delta = 5\%$, where Q_y and m are yield strength and mass of the system respectively. The figure confirm that

the input energy increases while the peak ground acceleration increases too. The identical phenomena was also observed in hysteretic energy spectra as shown in figure 2.

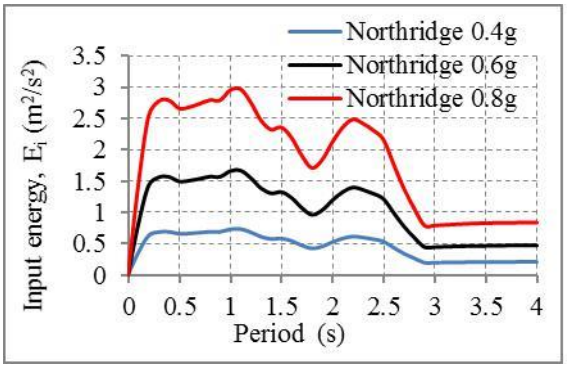

Figure 1. Influence of the PGA on the input energy spectra for SDOF under Northridge earthquake

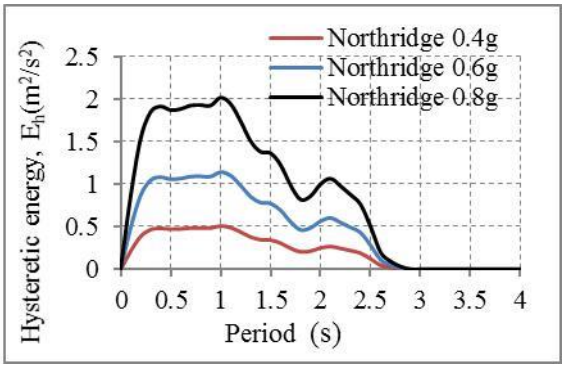

Figure 2. Influence of PGA to hysteretic energy spectra for the SDOF under Northridge earthquake.

2.2.2. Influence of strength ratio

Figure 3 present the input energy energy spectra of SDOF systems for damping ratio δ = 5%, bilinear model with post yield stiffness ratio = 0.04, and strength ratio 0.2, 0.4, and 0.6 subjected to Northridge earthquake of Arleta Nordhoff fire station scaled to 0.4g. It can be observed that strength ratio has a major effects on the input energy spectra, particularly close to predominant period. It was also noted that the predominant period of input energy spectra almost the same. The peak of the input energy spectra decreases with the decreasing of strength ratio. In addition, for long period region, the strength ratio does not have effects on the input energy spectra.

2.2.3. Influence of ductility ratio

The differential equation of motion for a general inelastic SDOF system can be expressed as:

$$m\ddot{u}(t) + c\dot{u}(t) + R(t) = -m\ddot{u}_g(t) \tag{9}$$

Normalized form differential equation of motion can be expressed as follows:

$$\ddot{\mu}(t) + \frac{4\pi}{T}\varsigma\dot{\mu}(t) + \frac{4\pi^2}{T^2}\rho(t) = -\frac{4\pi^2}{T^2\eta}\frac{\ddot{u}_g(t)}{\ddot{u}_{g,max}} \tag{10}$$

where μ (t) is displacement ductility of system, T is natural period, ς is damping ratio, and ρ (t) is the ratio inelastic restoring force R (t) to yield strength Qy of the and η is the strength ratio defined as relationship between system's yield strength and the maximum ground force applied during the motion. Figure 4 illustrates the influence of ductility factor μ to input energy for SDOF system, bilinear model, post yield stiffness ratio = 0.04, damping ratio ς = 5% subjected to Imperial Valley earthquake scaled to 0.35g. The figure reveal that ductility factor has significant influence on input energy spectra, in which input energy spectra decreases with the increasing of the ductility factor. Another interesting that, the predominant period of input energy spectra shorter with the increasing of the ductility factor, i.e. TPi = 0.9s for ductility factor μ = 1.0 decreases to be TPi = 0.51s for ductility factor μ = 6.0

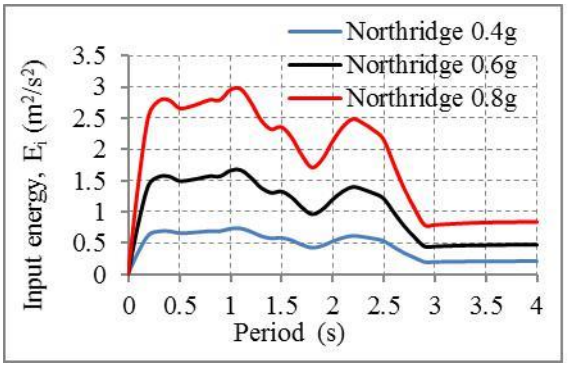

Figure 3. Comparison of input energy input energy spectra for SDOF system under Northridge earthquake with different strength ratio.

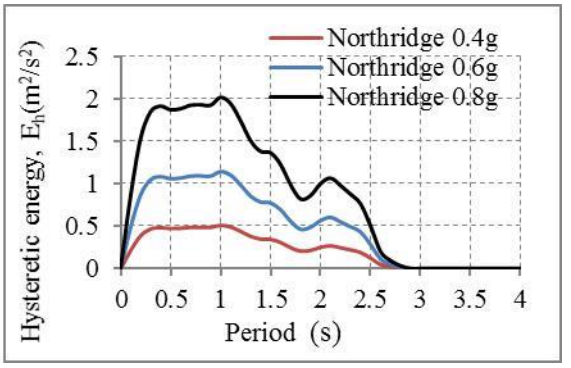

Figure 4. Comparison of input energy spectra for SDOF system under Imperial Valley earthquake with different ductility factor.

3. Damage Indices

During the last 20 years the concern in seismic design has been progressively change from force based to performance based. Damage occurred during earthquake seems to be seriously attention of the engineers of many countries, including developed countries, because of design building code may not adopted completely the seismic design philosophy. Currently, energy based approach are often used in earthquake resistant structures design. Riddle and Garcia [9] proposed the method to derive hysteretic energy dissipation spectra and application to damage control. Choi and Kim [4] developed energy seismic based design using hysteretic energy spectrum and accumulative ductility spectrum, Leelataviwat et al. [6] proposed performance plastic based design based on energy concept.

To investigate the damage potential of structure under seismic excitation, it is necessary to understand the correlation between energy demand parameters with structural response parameters. In this context, the energy demand parameters which also known as damage index are commonly accepted as indicator to measure damage state of structure. Damage index model based on cumulative plastic deformation and maximum hysteretic energy demand has been developed by several researcher, such as [7][8][5][2]. In this paper damage index model Park and Ang are introduced and employed to investigate the damage level of the building under consideration since the model more popular and give reasonably results.

3.1. Park and Ang Damage Model

Park and Ang [7], Park et al. [8] expressed damage index as a linear combination of the damage caused by excessive deformation and that contributed by cumulative plastic deformation, That is

$$DI = \frac{\delta_m}{\delta_u} + \beta \frac{E_h}{Q_y \delta_u} \tag{11}$$

where δ_m is the maximum deformation under seismic excitation; δu is the maximum deformation under monotonic loading; E_h is absorbed hysteretic energy; Q_y is yield strength of structure; and β is a parameter representing the damage contribution due to cyclic loading calibrated from experimental test. The better detailing and construction quality, the smaller constant β, the less potential of damage. The β factor have mean value of 0.15 for concrete structure, while for the steel structure Park et al.(1987) proposed β = 0.025. Here, DI is used as indicator of damage state of structures. When, DI ≥ 1.0 is assumed as condition of failure, and when DI = 0 indicate no structural damage (elastic). The value of DI in the range of between 0 < DI < 1.0, shows some measure of the degree of damage. However, this model has deficiency which related to physical meaning of damage index. When, E_h = 0 and damage index to be suppose zero, but according to Eq.(11) that the value of DI greater than zero. The interpretation of correlation between damage index and damage state of structure are listed in table 1.

Table 1. Interpretation of damage index

Degree of damage	Damage index	State of structure
Minor	0.0-0.2	Serviceable
Moderate	0.2-0.5	Reparable
Severe	0.5-1.0	Irreparable
collapse	>1.0	Loss of building

4. Numerical Study

4.1. Description of Investigated Building

To evaluate seismic performance of a structure based on energy concept under three selected earthquakes, an 4 (four) story of moment resisting frame (MRF) are considered as depicted in figure 5. In order to have the simulation more reasonable, the structure is designed to withstand realistic gravity load (dead load and live load). The magnitude of gravity load each story is assumed to be 32 kN/m. The pulse type ground motion records were used herein which is compatible to response spectra design of Indonesian Code 2013 as shown in Figure 6. The size of columns and beams member of MRF were designed based on capacity design concept and listed in table 2.

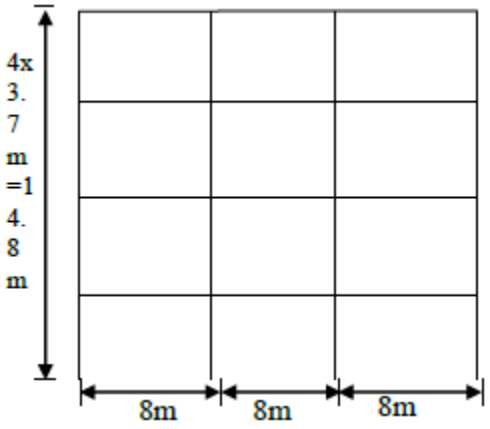

Figure 5. Schematic of MRF

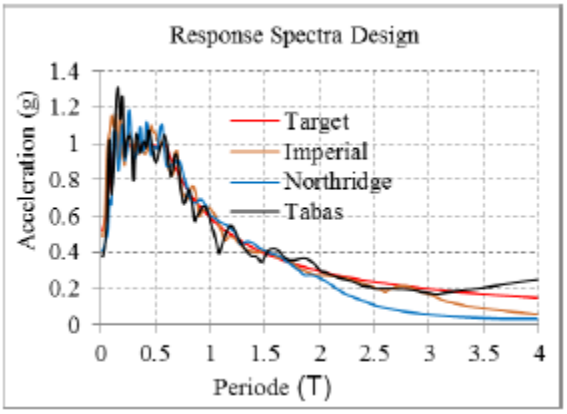

Figure 6. Response spectra of scaled ground motion with compatible SNI

Table 2. Dimension of columns and beams

	Columns dimension		Beams dimension	
	Interior	Exterior	Interior	Exterior
Story 1	W360x110	W360x101	W460x74	W460x74
Story 2	W360x101	W360x91	W460x74	W460x74
Story 3	W360x91	W360x79	W460x68	W460x68
Story 4	W360x79	W360x79	W460x60	W460x60

4.2. Structural Analysis And Modeling

The finite element analysis of the all frames subjected to three scaled up of acceleration records was conducted by use program ABAQUS. All beams and column were modeled as one dimensional element of the B21 beam element, and all connection columns to foundation were modeled as fixed support at ground level, while beam column joints were assumed perfectly rigid connection. Steel material was assumed to have an elastic modulus of 200 Gpa, an yield stress of 240 Mpa. The steel material for members assumed bilinear with strain hardening. The stress at 0.20 strain is assumed 360 Mpa. Isotropic hardening model were specified in order to take into account inelastic behavior of the element. Non-linier geometry option was also turn on for account second order effect which relate to P-delta and buckling. Rayleigh damping was constructed through the first and the fourth mode of vibration were specified 2% of critical damping.

5. Results And Discussion

5.1. Base Shear Demand

Base shear demands are depicted in Figure 7. The maximum base shear occurs under Tabas earthquake (666kN), while the smallest base shear occurs due to Imperial Valley earthquake (601kN). Although, seismic input and hysteretic energy under Northridge earthquake is less than Imperial valley earthquake, however the base shear demands induced by Northridge earthquake exhibit larger than Imperial valley earthquake. It means that there is no direct correlation between the seismic input energy and base shear. The main reason for this is the peak and predominant frequencies of the ground motion records under consideration are not equal, while the dynamic structure properties does not changed.

5.2. 5.2. Capacity Curve

Capacity curves of MRF frames which derived from nonlinear static pushover analysis are shown in figure 8. These figure provide information relate to the base shear and roof displacement relationship of those frames. Capacity curves for the MRF frames is constructed until failure. The failure condition occur when the frame met one of the following criteria , i.e. maximum story displacement on the roof is 4% of the building height or base shear total achieved 80% of the its peak value. It was found that ductility of MRF is $p = u / y = 6.5 \sim 4$. Therefore, evaluated building is categorized as ductile frame as expected in capacity design concept.

5.3. Time History Input And Hysteretic Energy Demand

Figure 9 and 10 show time history of input and hysteretic energy demand. Also, the ratio of maximum hysteretic energy to maximum input energy are listed in table 3. It was notable that time history of hysteretic energy is similar to time history of input energy. The larger of input energy transmitted to the systems, the larger of hysteretic energy absorbed by inelastic deformation of structural members. Tabas earthquake induced the largest input and hysteretic energy demands, while the lowest input and hysteretic energy demands is due to Northridge earthquake. The largest and the smallest ratio of maximum hysteretic energy to maximum input energy is 63.7% and 72.5%, respectively. Furthermore, the distribution of hysteretic energy over the height of building are plotted in Figure 11. It was noted that the distribution of hysteretic energy over the height of structure shows the same pattern. In addition, the maximum hysteretic energy demand occurs on the lowest floor.

Figure 9. Time histories of input energy

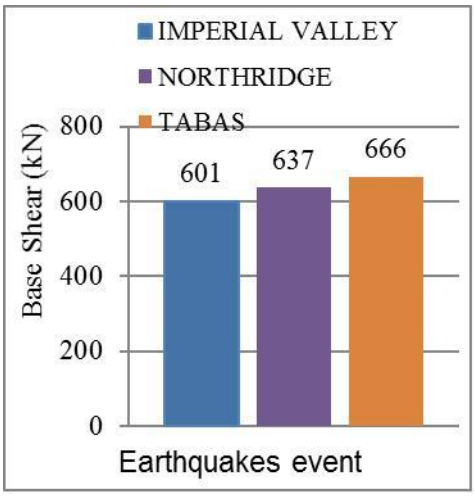

Figure 10. Time histories of hysteretic energy demand (E_H)

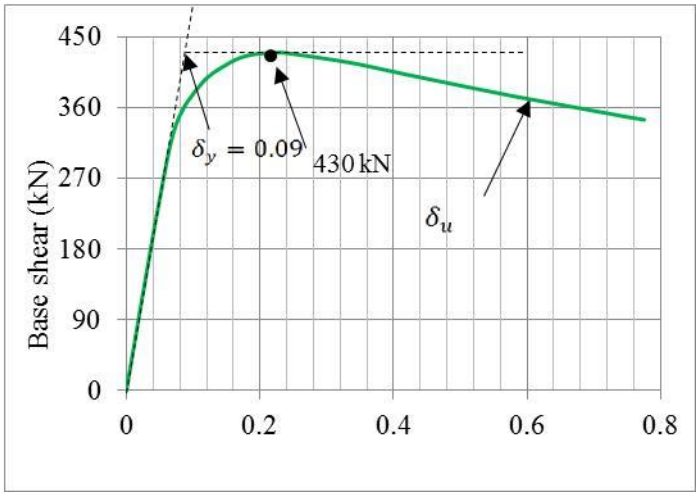

Table 3. Maximum input, hysteretic energy, and ratio of maximum hysteretic to input energy

Earthquakes	$E_I(N\text{-}m)x10^5$	$E_H(N\text{-}m)x10^5$	$E_H/E_I(\%)$
Imperial Valley	7.054	4.496	63.7
Northridge	4.1782	2.855	68.3
Tabas	8.112	5.849	72.1

Figure 11. Distribution of hysteretic energy demand (E_H)

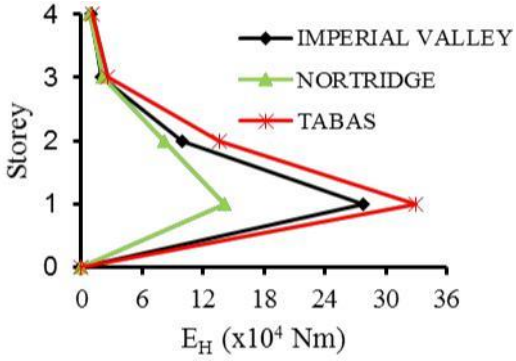

5.4. Story Drift

The story drift have been widely recognize as indicator of building performance level. Figure 12 and Figure 13 present the computed drift and story drift both positive and negative side over the height of frame, respectively. Maximum lateral displacement on the top floor is 234 mm due to Tabas earthquake, and the smallest is 169 mm under Northridge earthquake. In addition, there are correlation between input and hysteretic energy with story drift in which the higher input and hysteretic energy demands, the higher story drift and drift demands. Figure 13 display that the value of computed story drift almost the threshold of 2.5%, corresponding to the limit state of life safety (LS). The

maximum story drift is 2.33% due to Tabas earthquake. Figure 13 also shows that maximum story drift for Imperial valley and Northridge earthquakes occur on the second floor, while for Tabas earthquake occurs on the first floor. It means that under event Tabas earthquake the of maximum hysteretic energy demands and story drift demands occur at the same floor. In addition, the value of interstory drift correspondence with input and hysteretic energy total, also with (E_H / E_I) ratio as well.

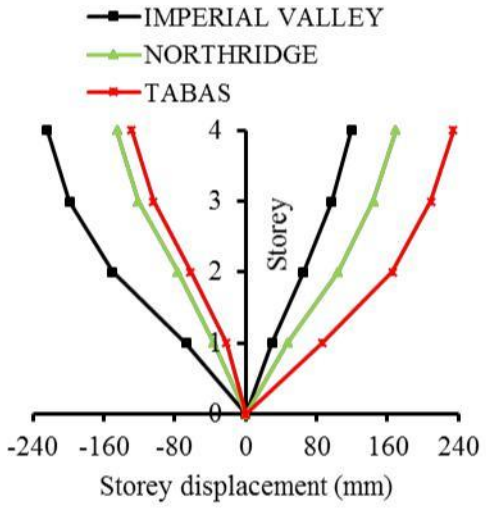

Figure 12 Story displacement for MRF

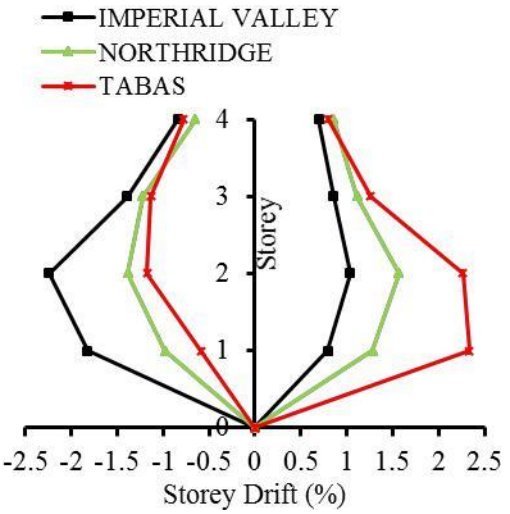

Figure 13 Story drift demand for MRF

5.5. Global Damage Index

One of response parameters commonly used as seismic performance indicator is story drift, although the lack of this parameter to predict damage induced by earthquake. According to the code when performing time history analysis of structure subjected to three acceleration records, story drift are taken as maximum response from the three analysis. Finally, the global damage index for MRF frame can be determined using Eq.(11) under Tabas earthquake, that is:

$$DI = \frac{\delta_m}{\delta_u} + \beta \frac{E_h}{Q_y \delta_u} = \frac{234}{600} + 0.025 \frac{584.9}{340x0.6} = 0.46$$

It was clearly that the seismic performance of the investigated building are expected at level repairable since $0.2 < DI < 0.5$. In addition, damage index also correlate well with story drift demand (2.33%) where the building assumed fall into life safety performance level.

6. Conclusions

Based on observation of the results obtained by nonlinear dynamic analysis, the following main conclusion can be drawn: the input energy induced by ground motion excitation influenced by characteristic of earthquakes and structural properties. Increased PGA followed by an increased in the input energy is transmitted into structure. Similar trends observed in the strength ratio. On the contrary, an increased in ductility ratio resulted in reductions in the input energy. The degree damage in a structure more closely relate to energy absorbed by structural component than the size of the applied force, and in a such a case, the influence of earthquake may be better expressed in term of energy than in term of force. Damage index can be used as alternative for interpretation the damage state of a structure, and can be associated with story drift index.

References

[1] ABAQUS. (2004). Standard/User‘s Manual, Version 10.1., Inc. USA
[2] Bojórquez, E., Reyes-Salaza, A., Terán-Gilmore, A., and Ruiz, S.E. (2010). Energy-based damage index for steel structures , Steel and Composite Structures 4(4), 343-360.
[3] Chao, S.-H., and Goel, S. C.(2005). ―Performance-Based Seismic Design of EBF UsingTarget Drift and Yield Mechanism as Performance Criteria," Report No. UMCEE 05-05, Department of Civil and Environmental Engineering, University of Michigan,
[4] Choi, H., and J. Kim, (2006). Energy-based seismic design of buckling-restrained braced frames using hysteretic energy spectrum, Engineering Structures 28, 304-311.
[5] Cosenza, E., Manfredi, G. and Ramasco, R. (1993). The use of damage functional in earthquake engineering: a comparison between different methods, Earthquake Engineering and Structural Dynamics 22, 855–868
[6] Leelataviwat, S., Saewon, W., Goel, S.C. (2008)." An energy base method for seismic evaluation of structure". The 14th World Conference on Earthquake Engineering, Beijing, China.
[7] Park, Y.J. and Ang, A.H. (1985), Mechanistic seismic damage model for reinforced concrete, J. Struct. Eng. ASCE, 111(4), 740-757.
[8] Park, Y. J., Ang, A. H.-S., and Wen, Y. K. (1987). Damage-limiting aseismic design of buildings. Earthquake Spectra, 3(1), 1–26.
[9] Riddle, R.,Garcia, J.E. (2001). Hysteretic energy spectrum and damage control. Earthquake Engineeringand Structural Dynamics,30(12):1781~1791
[10] Uang, C. M. and V. V. Bertero, (1990). Evaluation of seismic energy in structures. Earthquake Engineering and Structural Dynamics 19, 77-90.
[11] Zahrah, T. F. and Hall, W. J. (1984). Earthquake energy absorption in SDOF structures, ASCE Journal of Structural Engineering, 110(8), 1757–1772.